Journal of Sound and Vibration 411 (2017) 88–107

Contents lists available at ScienceDirect

Journal of Sound and Vibration

journal homepage: www.elsevier.com/locate/jsvi

Dynamic output feedback control for seismic-excited buildings

Ali Kazemy [a], Xian-Ming Zhang [b], Qing-Long Han [b,*]

[a] Department of Electrical Engineering, Tafresh University, Tafresh, 39518-79611, Iran
[b] School of Software and Electrical Engineering, Swinburne University of Technology, Melbourne, VIC, 3122, Australia

ARTICLE INFO

Article history:
Received 1 April 2017
Revised 26 July 2017
Accepted 12 August 2017
Available online XXX

Keywords:
Building structures
$\mathcal{H}_\infty$ control
Dynamic output feedback
Earthquake

ABSTRACT

This paper deals with the $\mathcal{H}_\infty$ dynamic output feedback control problem of a seismic-excited building. The control aims to reduce the vibration of a building caused by an earthquake. Instead of system states, the system output measurements are used to design suitable $\mathcal{H}_\infty$ controllers. Depending on whether the system measurements are sampled or not, two kinds of dynamic output feedback control schemes are investigated. By the Lyapunov stability theory, some bounded real lemmas are formulated such that the closed-loop system is asymptotically stable and achieves a prescribed $\mathcal{H}_\infty$ disturbance attenuation level. The cone complementary algorithm is employed to design $\mathcal{H}_\infty$ controllers based on a solution to a nonlinear minimization problem subject to a set of linear matrix inequalities. Finally, a three-storey building model is given to show the effectiveness of the proposed method.
© 2017 Elsevier Ltd. All rights reserved.

1. Introduction

An earthquake is a natural disaster that usually causes serious damage and destruction of buildings. Thus, it is important to develop effective methods of construction against earthquakes, especially for high-rise buildings due to their inherent susceptibility from earthquakes. Up to date, several methods are proposed to protect buildings against earthquakes, which can be classified into three categories: passive control, semi-active control, and active control. Tuned-mass-dampers (TMD), base isolations, friction and viscous dampers, and structural energy dissipation devises are some examples of passive control techniques [1–5]. Changing the structural parameters such as damping and stiffness is a kind of semi-active control technique [6–8]. Pumping energy to structure by using appropriate actuators is regarded as an active control method [9–11]. Since the effectiveness, this paper focuses on developing an active control method against earthquakes.

The active control of structures was first implemented in Kyobashi Center Building in 1989. Since then, several active control methods are proposed, e.g., for vibration control of buildings [9–14]. Active controllers are designed usually using optimal control methods [7,15,16], robust control methods for the structures in presence of structured and unstructured uncertainties [17–19], and intelligent control methods based on neural networks and fuzzy systems [13,20–22]. Classical control methods such as PID control and sliding mode control are also used to design active controllers [22–24]. The $\mathcal{H}_\infty$ control method is a well-known optimal control strategy that has been used for many years as well as applied for active control of building structures [25–27]. It is worth pointing out that earthquakes have finite frequency spectrum characters, based on which, $\mathcal{H}_\infty$ control for buildings under earthquake excitation is studied [28]. Moreover, active fault tolerant control of buildings is also investigated for seismic loads in finite frequency domain, and recently, equivalent-input-disturbance and energy-to-peak control of structures are proposed [29–31]. However, most methods mentioned above are based on such an assumption that the system state is

* Corresponding author.
E-mail addresses: kazemy@tafreshu.ac.ir (A. Kazemy), xianmingzhang@swin.edu.au (X.-M. Zhang), qhan@swin.edu.au (Q.-L. Han).

http://dx.doi.org/10.1016/j.jsv.2017.08.017
0022-460X/© 2017 Elsevier Ltd. All rights reserved.

available. This assumption cannot be satisfied for some practical systems due to that only measurement outputs can be used for control design. Thus, it is significant to develop an effective method to design output feedback controllers, especially in the case where system states are not available, which motivates the present study.

In general, there are two ways for measurement signals to be transmitted from a building to a controller: analog signal transmission and digital signal transmission [32–34]. Traditionally, analog signal transmission requires wirings to connect a building to a controller. When the building and the controller are located in the same place, analog signal transmission is a good way to transmit signals from the building to the controller continuously such that some better closed-loop performance can be achieved. However, it is possible that the building and the controller are not located at the same place due to the fact that nobody knows which buildings will suffer earthquakes when earthquakes happen. In this situation, digital signal transmission comes to the fore, in which measurement signals are sampled first in a digital form and then transmitted to the controller through a communication network. Compared with analog signal transmission, digital signal transmission has several advantages, such as no wirings, high reliability, high signal-to-noise ratio (SNR) and suitability for sending data to long distances [35,36]. With the rapid development of communication technology, modern industrial applications are based on digital signal transmission rather than analog signal transmission.

In this paper, two kinds of dynamic output feedback control schemes are investigated for seismic-excited buildings. When the building and the controller are located at the same place, a continuous-signal-based dynamic output feedback control scheme is devised using analog signal transmission. When the building and the controller are located at different places, a sampled-data-based dynamic output feedback control scheme is presented with digital signal transmission. By employing Lyapunov-Krasovskii stability theory, some sufficient conditions on the existence of suitable dynamic output feedback controllers are derived in terms of the solution to a nonlinear minimization problem subject to linear matrix inequalities. Simulation results demonstrate the effectiveness of the proposed control schemes.

This paper is organized as follows. Section 2 describes the dynamic model of n-DOF seismic-excited building. Some useful lemmas are also provided in this section. Two methods are presented in Section 3 to design suitable dynamic output feedback controllers. The simulation results and some comparison with other methods are given in Section 4. Section 5 concludes the paper, and the proofs of theorems proposed in this paper are provided in Appendix.

Notations. The notation in this paper is standard. A symmetric term in a symmetric matrix is denoted by $*$.

2. Problem statement

Consider a typical n-DOF building model shown in Fig. 1 [34]. The motion equations of the seismic-excited building can be obtained by the Newton's second law, which is given as

$$\mathbf{M}_0\ddot{\mathbf{q}}(t) + \mathbf{C}_0\dot{\mathbf{q}}(t) + \mathbf{K}_0\mathbf{q}(t) = \mathbf{H}_0\mathbf{u}(t) + \xi_0\ddot{x}_g(t), \tag{1}$$

where $\mathbf{q}(t) = \mathrm{col}\{q_1(t), q_2(t), \ldots, q_n(t)\} \in \mathbb{R}^n$ denotes the inter-storey relative drift vector between the floors, and $q_i(t)$ is the relative drift between the ith and the $(i-1)$th floor; $\mathbf{u}(t) = \mathrm{col}\{u_1(t), u_2(t), \ldots, u_n(t)\} \in \mathbb{R}^n$ is the control force vector produced by n actuators, with each of them installed at the bottom of each storey; $\ddot{x}_g(t) \in \mathbb{R}$ represents the ground acceleration caused by the earthquake. $\mathbf{H}_0$ is an $n \times n$ real matrix; and the matrices $\mathbf{M}_0$, $\mathbf{C}_0$, $\mathbf{K}_0$ and the vector $\boldsymbol{\xi}_0$ are given by

$$\mathbf{M}_0 = \begin{bmatrix} m_1 & 0 & 0 & \cdots & 0 \\ m_2 & m_2 & 0 & \cdots & 0 \\ \vdots & \vdots & \ddots & \ddots & \vdots \\ m_{n-1} & m_{n-1} & m_{n-1} & \ddots & 0 \\ m_n & m_n & m_n & \cdots & m_n \end{bmatrix}, \quad \mathbf{C}_0 = \begin{bmatrix} c_1 & -c_2 & 0 & \cdots & 0 \\ 0 & c_2 & -c_3 & \ddots & \vdots \\ \vdots & \ddots & \ddots & \ddots & 0 \\ \vdots & & \ddots & c_{n-1} & -c_n \\ 0 & \cdots & \cdots & 0 & c_n \end{bmatrix}$$

$$\mathbf{K}_0 = \begin{bmatrix} k_1 & -k_2 & 0 & \cdots & 0 \\ 0 & k_2 & -k_3 & \ddots & \vdots \\ \vdots & \ddots & \ddots & \ddots & 0 \\ \vdots & & \ddots & k_{n-1} & -k_n \\ 0 & \cdots & \cdots & 0 & k_n \end{bmatrix}, \quad \xi_0 = \begin{bmatrix} -m_1 \\ -m_2 \\ \vdots \\ -m_n \end{bmatrix}$$

where the parameters m_i, c_i, and k_i, $(i = 1,2, \ldots, n)$ are the mass, damping, and stiffness of each storey, respectively.

Let $\mathbf{x}(t) = \mathrm{col}\{\mathbf{q}(t), \dot{\mathbf{q}}(t)\}$ and $w(t) = \ddot{x}_g(t)$. Then the state space representation of (1) can be given as

$$\dot{\mathbf{x}}(t) = \mathbf{A}\mathbf{x}(t) + \mathbf{B}\mathbf{u}(t) + \mathbf{F}w(t), \tag{2}$$

where

$$\mathbf{A} = \begin{bmatrix} \mathbf{0} & \mathbf{I} \\ -\mathbf{M}_0^{-1}\mathbf{K}_0 & -\mathbf{M}_0^{-1}\mathbf{C}_0 \end{bmatrix}, \quad \mathbf{B} = \begin{bmatrix} \mathbf{0} \\ \mathbf{M}_0^{-1}\mathbf{H}_0 \end{bmatrix}, \quad \mathbf{F} = \begin{bmatrix} \mathbf{0} \\ \mathbf{M}_0^{-1}\xi_0 \end{bmatrix}$$

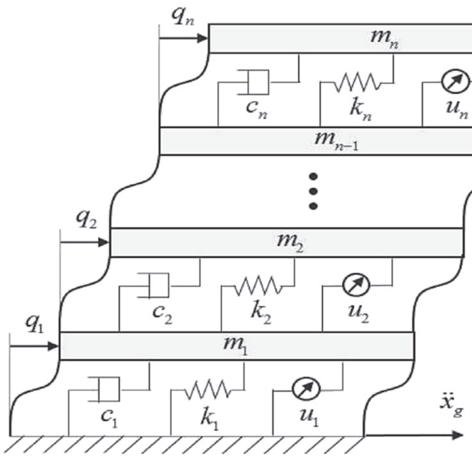

Fig. 1. A typical n-DOF building model.

In system (2), **w(t)** is an input disturbance, which is assumed to belong to $\mathcal{L}_2[0,\infty)$ with limited energy [28]. In this paper, we focus on designing an $\mathcal{H}_\infty$ controller via dynamic output feedback. In doing so, the measurement output $\mathbf{y}(t) \in \mathbb{R}^r$ and the controlled output $\mathbf{z}(t) \in \mathbb{R}^p$ are supposed to be of form

$$\begin{cases} \mathbf{y}(t) = \mathbf{C}_1\mathbf{x}(t), \\ \mathbf{z}(t) = \mathbf{C}_2\mathbf{x}(t), \end{cases} \tag{3}$$

where the matrix $\mathbf{C}_1 \in \mathbb{R}^{r\times 2n}$ depends on sensor types, velocity or displacement and their locations, and the matrix $\mathbf{C}_2 \in \mathbb{R}^{p\times 2n}$ is chosen to improve the control performance of the resultant closed-loop system, which will be discussed in the section of simulation.

The objective of the paper is to design a dynamic output feedback controller for the seismic-excited building (2) and (3), such that the resultant closed-loop system is internally asymptotically stable and satisfies

$$\int_0^\infty \|\mathbf{z}(t)\|^2 dt \le \gamma^2 \int_0^\infty \|\mathbf{w}(t)\|^2 dt, \tag{4}$$

for any non-zero $w(t) \in \mathcal{L}_2[0,\infty)$ under zero initial conditions, where $\gamma > 0$ is a certain disturbance attenuation level and $\|.\|$ denotes the Euclidean norm.

Remark 1. From (3) and (4), it is clear that tuning the matrix $\mathbf{C}_2$ can improve the control performance. In fact, the emphasis can be placed on some storeys' displacement by choosing the appropriate matrix $\mathbf{C}_2$ in order to achieve some better control performance. In other words, taking into account the first floor for short buildings and the middle floor for high buildings usually yields better results. This will be further discussed in the simulation.

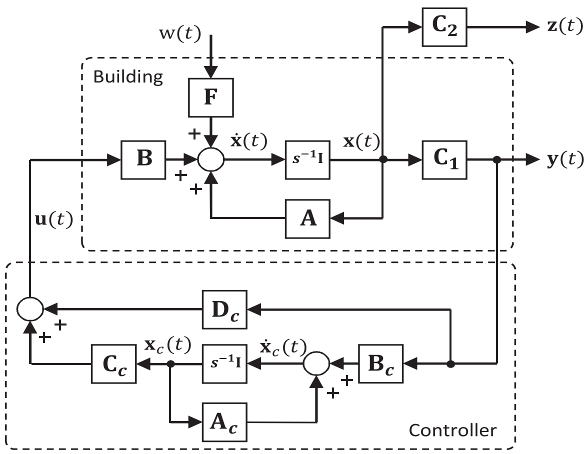

Fig. 2. The block diagram of the control system.

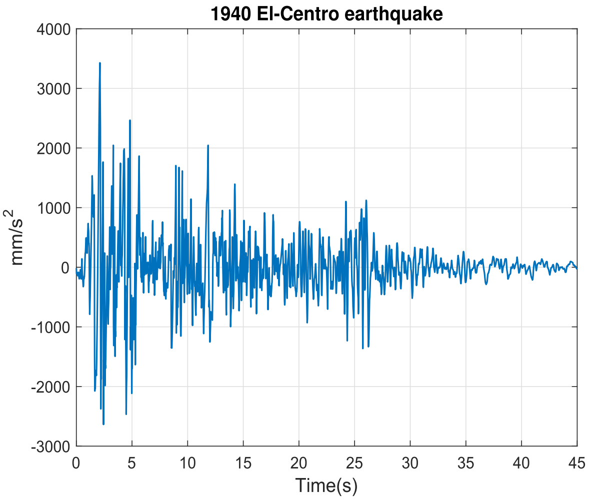

Fig. 3. 1940 El-Centro earthquakes real data for the input disturbance $w(t)$.

The following lemmas are useful in deriving the main results of the paper [37].

Lemma 1. (*A projection lemma*). *Let a symmetric matrix* $\mathbf{\Psi} \in \mathbb{R}^{n\times n}$, *two matrices* $\mathbf{P} \in \mathbb{R}^{n\times m}$ *and* $\mathbf{Q} \in \mathbb{R}^{k\times n}$ *be given. There exists a compatible real matrix* $\boldsymbol{X}$ *such that*

$$\mathbf{\Psi} + \mathbf{P}\mathbf{X}\mathbf{Q}^T + \mathbf{Q}\mathbf{X}^T\mathbf{P}^T < 0, \tag{5}$$

if and only if

$$\mathbf{P}_\perp^T\mathbf{\Psi}\mathbf{P}_\perp < 0, \tag{6}$$

$$\mathbf{Q}_\perp^T\mathbf{\Psi}\mathbf{Q}_\perp < 0, \tag{7}$$

hold, where $\mathbf{P}_\perp$ *and* $\mathbf{Q}_\perp$ *are the orthogonal complements of* $\mathbf{P}$ *and* $\mathbf{Q}$, *respectively.*

Lemma 2. ([38]) *Let* $\mathbf{X} \in \mathbb{R}^{n\times n}$ *and* $\mathbf{Y} \in \mathbb{R}^{n\times n}$ *be symmetric, positive definite matrices. Then, there exists a symmetric positive definite matrix* $\boldsymbol{P} > 0$ *satisfying*

$$\mathbf{P} = \begin{bmatrix} \mathbf{Y} & \# \\ \# & \# \end{bmatrix}, \quad \mathbf{P}^{-1} = \begin{bmatrix} \mathbf{X} & \# \\ \# & \# \end{bmatrix}$$

if and only if $\mathbf{X} - \mathbf{Y}^{-1} \geq \mathbf{0}$, *where '#' stands for some irrelative matrices.*

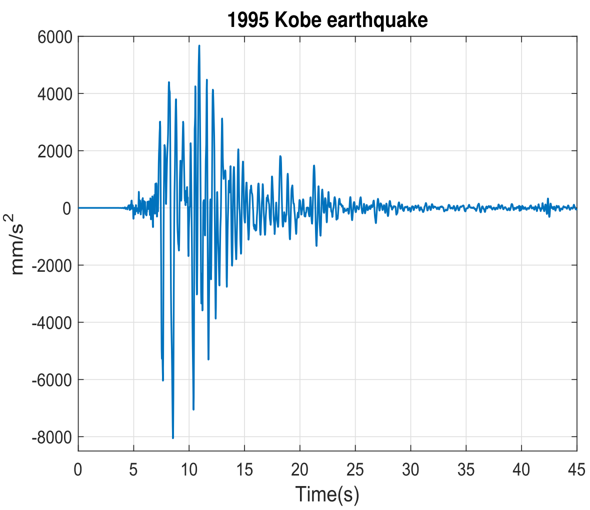

Fig. 4. 1995 Kobe earthquakes real data for the input disturbance $w(t)$.

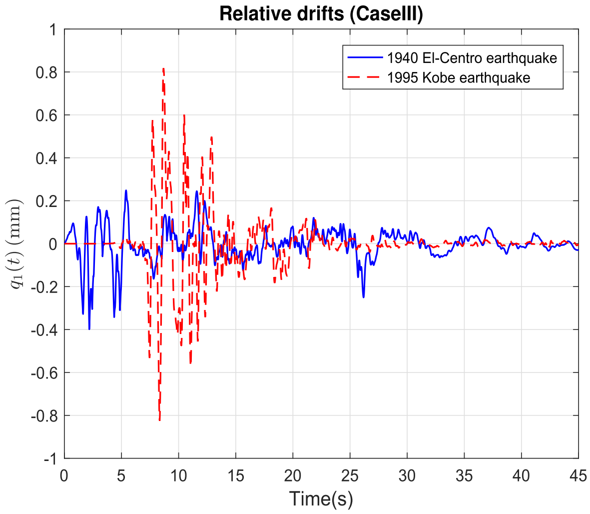

Fig. 5. The response of relative drifts in Case III to two earthquakes.

3. Design of dynamic output feedback controllers

In this section, two schemes are presented to design suitable dynamic output feedback controllers for the building model (2). One is based on the continuous measurement output signals, and the other on sampled-data measurement output signals.

3.1. Continuous-signal-based dynamic output feedback control

If the controller and the building are located at the same place, measurement output signals can be transmitted continuously from the building to the controller. Thus, the block diagram of the control system can be described in Fig. 2, where the controller to be designed is a dynamic output feedback controller of the following form

$$\begin{cases} \dot{\mathbf{x}}_c(t) = \mathbf{A}_c\mathbf{x}_c(t) + \mathbf{B}_c\mathbf{y}(t) \\ \mathbf{u}(t) = \mathbf{C}_c\mathbf{x}_c(t) + \mathbf{D}_c\mathbf{y}(t) \end{cases} \tag{8}$$

where $\mathbf{x}_c \in \mathbb{R}^{2n}$ is the state vector of the controller, and $\mathbf{A}_c \in \mathbb{R}^{2n\times 2n}$, $\mathbf{B}_c \in \mathbb{R}^{2n\times r}$, $\mathbf{C}_c \in \mathbb{R}^{m\times 2n}$, $\mathbf{D}_c \in \mathbb{R}^{m\times r}$ are the constant controller gain matrices to be designed. Introduce an augmented vector as

$$\boldsymbol{\xi}(t) = \mathrm{col}\left\{\mathbf{x}(t), \mathbf{x}_c(t)\right\}.$$

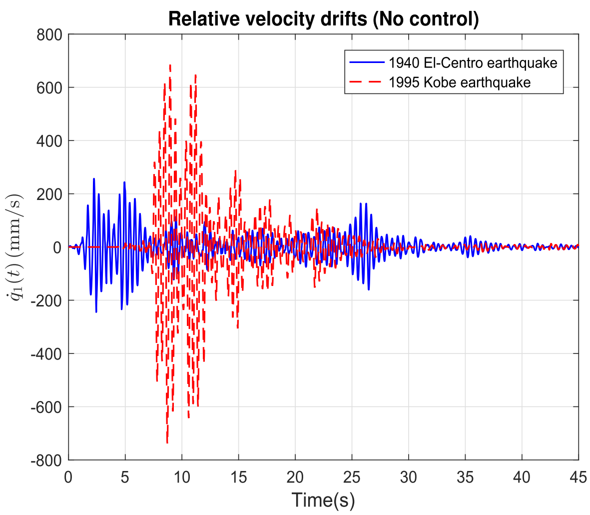

Fig. 6. The open-loop responses in Case III of relative velocity drifts to two earthquakes.

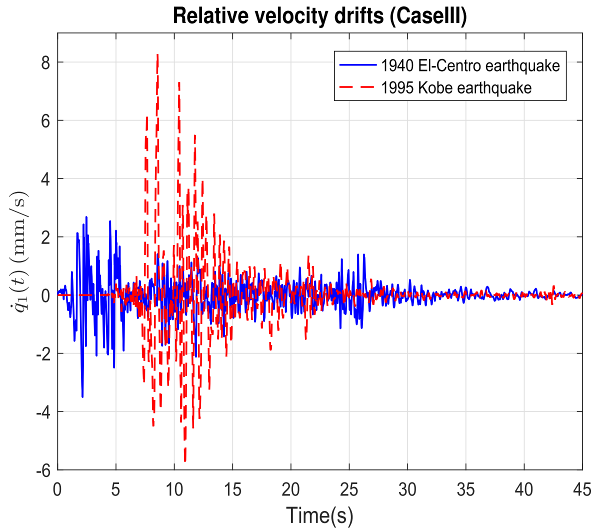

Fig. 7. The closed-loop responses in Case III of relative velocity drifts to two earthquakes.

Then we have

$$\dot{\xi}(t) = \left(\mathbf{A}_0 + \mathbf{HKL}\right)\xi(t) + \mathbf{E}^T\mathbf{F}w(t), \tag{9}$$

where $\mathbf{E} = [\mathbf{I}, \quad \mathbf{0}]$, and

$$\mathbf{A}_0 = \begin{bmatrix} \mathbf{A} & \mathbf{0} \\ \mathbf{0} & \mathbf{0} \end{bmatrix}, \quad \mathbf{H} = \begin{bmatrix} \mathbf{B} & \mathbf{0} \\ \mathbf{0} & \mathbf{I} \end{bmatrix}, \quad \mathbf{L} = \begin{bmatrix} \mathbf{C}_1 & \mathbf{0} \\ \mathbf{0} & \mathbf{I} \end{bmatrix}, \quad \mathbf{K} = \begin{bmatrix} \mathbf{D}_c & \mathbf{C}_c \\ \mathbf{B}_c & \mathbf{A}_c \end{bmatrix}. \tag{10}$$

The following theorem provides a bounded real lemma for the closed-loop system (9).

Theorem 1. *For a given $\gamma > 0$, the closed-loop system (9) is asymptotically stable and satisfies (4) if there exist a matrix $\mathbf{K} \in \mathbb{R}^{(2n+m)\times(2n+r)}$ and $\mathbf{P} \in \mathbb{R}^{2n\times 2n}$ with $\mathbf{P} > 0$ such that*

$$\mathbf{\Phi} := \begin{bmatrix} \mathbf{\Pi}_1 & \mathbf{PE}^T\mathbf{F} \\ * & -\gamma^2\mathbf{I} \end{bmatrix} < 0 \tag{11}$$

where $\mathbf{\Pi}_1 = \mathbf{P}\left(\mathbf{A}_0 + \mathbf{HKL}\right) + \left(\mathbf{A}_0 + \mathbf{HKL}\right)^{\mathbf{T}}\mathbf{P} + \mathbf{E}^{\mathbf{T}}\mathbf{C}_2^{\mathbf{T}}\mathbf{C}_2\mathbf{E}$.

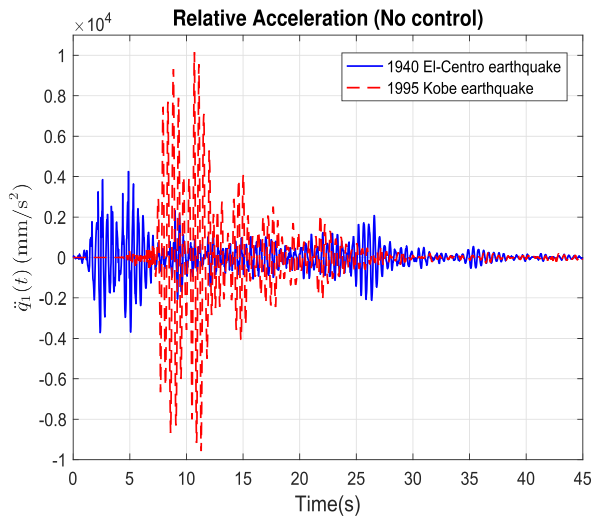

Fig. 8. The open-loop responses in Case III of relative acceleration to two earthquakes.

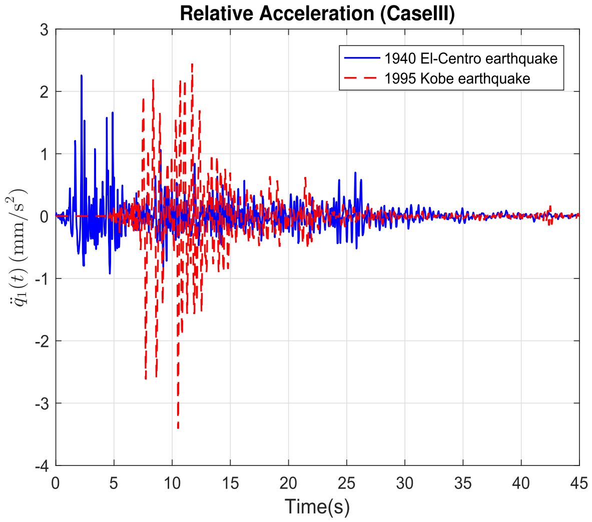

Fig. 9. The closed-loop responses in Case III of relative acceleration to two earthquakes.

Proof. *See Appendix A.* □

Theorem 1 presents a bounded real lemma for (9). However, it cannot be used directly to design suitable $\mathcal{H}_\infty$ controllers due to the nonlinear term **PHKL**. In order to deal with the nonlinear terms, using Lemma 1, the matrix inequality (11) is converted as an equivalent form as follows.

Theorem 2. *For a given $\gamma > 0$, there exist a matrix $\mathbf{K} \in \mathbb{R}^{(2n+m)\times(2n+r)}$ and a positive definite matrix $\mathbf{P} \in \mathbb{R}^{2n\times 2n}$ such that (11) if and only if there exist two positive definite matrices $\mathbf{X} \in \mathbb{R}^{n\times n}$ and $\mathbf{Y} \in \mathbb{R}^{n\times n}$ such that*

$$\begin{bmatrix} \mathbf{W}_1^T\left(\mathbf{AX}+\mathbf{XA}^T+\gamma^{-2}\mathbf{FF}^T\right)\mathbf{W}_1 & \mathbf{W}_1^T\mathbf{XC}_2^T \\ * & -\mathbf{I} \end{bmatrix} < 0 \tag{12}$$

$$\begin{bmatrix} \mathbf{W}_2^T\left(\mathbf{YA}+\mathbf{A}^T\mathbf{Y}+\mathbf{C}_2^T\mathbf{C}_2\right)\mathbf{W}_2 & \mathbf{W}_2^T\mathbf{YF} \\ * & -\gamma^2\mathbf{I} \end{bmatrix} < 0 \tag{13}$$

$$\begin{bmatrix} \mathbf{X} & \mathbf{I} \\ * & \mathbf{Y} \end{bmatrix} > 0 \tag{14}$$

where $\mathbf{W}_1$ and $\boldsymbol{W}_2$ are the orthogonal complements of $\boldsymbol{B}$ and $\mathbf{C}_1^T$, respectively.

Proof. *See Appendix B.* □

Based on Theorem 2, we can design suitable $\mathcal{H}_\infty$ controllers of form (8) using Algorithm 1 below.

Algorithm 1
1: Choose a small performance level $\gamma > 0$;
2: Find a feasible solution **X** and **Y** satisfying (12)–(14);
3: Calculate by the singular value decomposition $\mathbf{M} \in \mathbb{R}^{n\times n}$ and $\mathbf{N} \in \mathbb{R}^{n\times n}$ such that $\mathbf{MN}^T = \mathbf{I} - \mathbf{XY}$;
4: Compute the matrix P by solving the linear equation
$$\mathbf{P} = \begin{bmatrix} \mathbf{Y} & \mathbf{I} \\ \mathbf{N}^T & \mathbf{0} \end{bmatrix}\begin{bmatrix} \mathbf{I} & \mathbf{X} \\ \mathbf{0} & \mathbf{M}^T \end{bmatrix}^{-1};$$
5: With the obtained **P**, solve the feasible problem (11) to get **K**;
6: If there is no feasible solution, change the value of $\gamma > 0$ and go to step 2.

3.2. Sampled-data-based dynamic output feedback $\mathcal{H}_\infty$ control

For the practical point of view, especially when the system and the controller are located in different places, the measurement output needs to be first sampled and then transmitted to the controller in the digital form [39–41]. Once the controller receives the sampled signal, a control signal is immediately generated and is sent to activate the system. Suppose that the measured outputs $\mathbf{y}(t)$ are sampled at the time instants $0 < t_0 < t_1 < \cdots < t_k < t_{k+1} < \cdots$ with $\max\{t_{k+1} - t_k | k = 0, 1, 2, \cdots\} \le h$, where h is a known positive constant. Then

$$\mathbf{y}(t) = \mathbf{y}(t_k), \quad t_k \le t < t_{k+1}, \tag{15}$$

We design the dynamic output feedback controller as

$$\begin{cases} \dot{\mathbf{x}}_c(t) = \mathbf{A}_c\mathbf{x}_c(t) + \mathbf{B}_c\mathbf{y}(t_k) \\ \mathbf{u}(t) = \mathbf{C}_c\mathbf{x}_c(t) + \mathbf{D}_c\mathbf{y}(t_k) \end{cases}, t_k \le t < t_{k+1} \tag{16}$$

where $\mathbf{x}_c(t) \in \mathbb{R}^{2n}$, and the matrices $\mathbf{A}_c \in \mathbb{R}^{2n\times 2n}$, $\mathbf{B}_c \in \mathbb{R}^{2n\times r}$, $\mathbf{C}_c \in \mathbb{R}^{m\times 2n}$, $\mathbf{D}_c \in \mathbb{R}^{m\times r}$, are the constant controller gain matrices to be designed. Define a saw-tooth function as

$$d(t) = t - t_k, \quad t_k \le t < t_{k+1},$$

which satisfies

$$0 \le d(t) < h$$

Thus, the dynamic output feedback controller (16) becomes

$$\begin{cases} \dot{\mathbf{x}}_c(t) = \mathbf{A}_c\mathbf{x}_c(t) + \mathbf{B}_c\mathbf{y}(t - d(t)) \\ \mathbf{u}(t) = \mathbf{C}_c\mathbf{x}_c(t) + \mathbf{D}_c\mathbf{y}(t - d(t)) \end{cases} \tag{17}$$

Denote $\boldsymbol{\xi}(t) = \mathrm{col}\{\mathbf{x}(t), \mathbf{x}_c(t)\}$. Then the resultant closed-loop system associated with (2) and (17) can be given by

$$\dot{\boldsymbol{\xi}}(t) = \left(\mathbf{A}_0 + \mathbf{HKL}_1\right)\boldsymbol{\xi}(t) + \mathbf{HKL}_2\boldsymbol{\xi}(t - d(t)) + \mathbf{E}^T\mathbf{F}w(t), \tag{18}$$

where $\mathbf{A}_0$, $\mathbf{H}$, $\mathbf{E}$, and $\mathbf{K}$ are given in (9) and (10), and $\mathbf{L}_1 = \mathrm{diag}\{\mathbf{0}, \mathbf{I}\}$, $\mathbf{L}_2 = [\mathbf{C}_1^T, \mathbf{0}]^T$.

We now state and establish a bounded real lemma for the closed-loop system (18).

Theorem 3. *For given scalars $\gamma > 0$ and $h > 0$, the closed-loop system (18) is asymptotically stable with (4) being satisfied, if there exist $\mathbf{K} \in \mathbb{R}^{(2n+m)\times(2n+r)}$, matrices $\mathbf{P} \in \mathbb{R}^{2n\times 2n}$ with $P > 0$, $\mathbf{Q} \in \mathbb{R}^{n\times n}$ with $\mathbf{Q} > 0$, and $\mathbf{R} \in \mathbb{R}^{n\times n}$ with $R > 0$ such that*

$$\overline{\boldsymbol{\Phi}} = \begin{bmatrix} \boldsymbol{\Xi}_1 & \boldsymbol{\Xi}_2 & \mathbf{0} & \mathbf{PE}^T\mathbf{F} & h\left(\mathbf{A}_0 + \mathbf{HKL}_1\right)^T\mathbf{E}^T\mathbf{R} \\ * & -2\mathbf{R} & \mathbf{R} & \mathbf{0} & h\left(\mathbf{HKL}_2\right)^T\mathbf{E}^T\mathbf{R} \\ * & * & -\mathbf{Q}-\mathbf{R} & \mathbf{0} & \mathbf{0} \\ * & * & * & -\gamma^2\mathbf{I} & h\mathbf{F}^T\mathbf{R} \\ * & * & * & * & -\mathbf{R} \end{bmatrix} < 0 \tag{19}$$

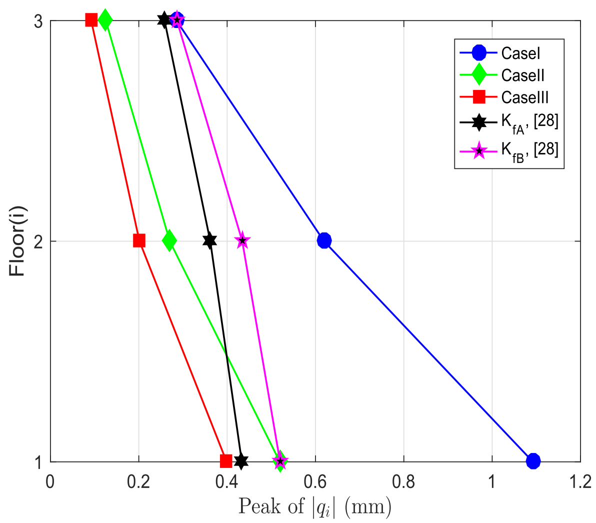

Fig. 10. Comparison results for $|q_i|$ ($i = 1,2,3$) under the 1940 El-Centro earthquakes.

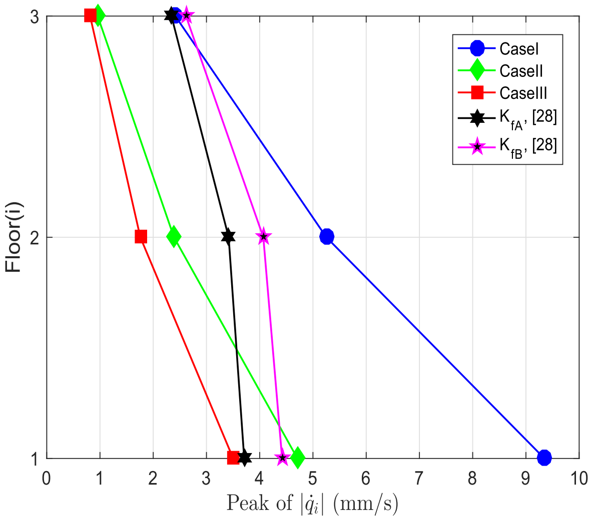

Fig. 11. Comparison results for $|\dot{q}_i|$ $(i = 1,2,3)$ under the 1940 El-Centro earthquakes.

where $\Xi_1 = \mathbf{P}\left(\mathbf{A}_0 + \mathbf{HKL}_1\right) + \left(\mathbf{A}_0 + \mathbf{HKL}_1\right)^T\mathbf{P} + \mathbf{E}^T\mathbf{QE} - \mathbf{E}^T\mathbf{RE} + \mathbf{E}^T\mathbf{C}_2^T\mathbf{C}_2\mathbf{E}$, $\Xi_2 = \mathbf{PHKL}_2 + \mathbf{E}^T\mathbf{R}$.

Proof. *See* Appendix C. □

Due to existence of nonlinear terms in (19), the controller gain $\mathbf{K}$ cannot be easily solved out from Theorem 3. An equivalent version to (19) is presented as follows.

Theorem 4. *For given constants* $\gamma > 0$ *and* $h > 0$, *there exists a real matrix* $\boldsymbol{K}$ *such that the matrix inequality* (19) *is satisfied if and only if there exist* $n \times n$ *real matrices* $\boldsymbol{X} > 0$, $\boldsymbol{Y} > 0$, $\boldsymbol{Q} > 0$ *and* $\boldsymbol{R} > 0$ *such that*

$$\mathbf{\Gamma} = \begin{bmatrix} \mathbf{\Psi} & \mathbf{W}_1^T\mathbf{XR} & \mathbf{0} \\ * & -2\mathbf{R} & \mathbf{R} \\ * & * & -\mathbf{Q} - \mathbf{R} \end{bmatrix} < 0, \tag{20}$$

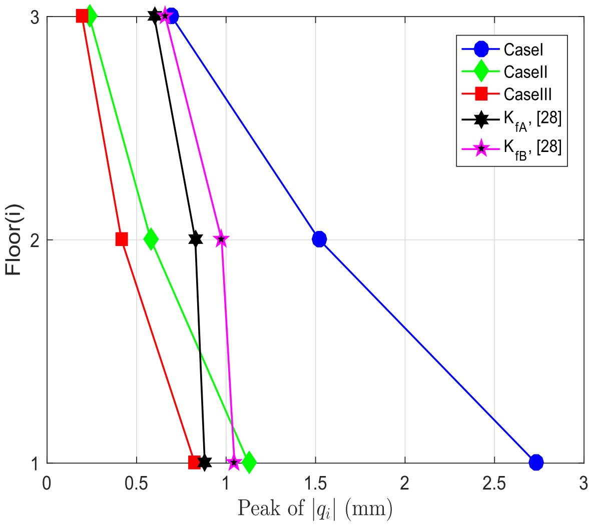

Fig. 12. Comparison results for $|q_i|$ $(i = 1,2,3)$ under the 1995 Kobe earthquakes.

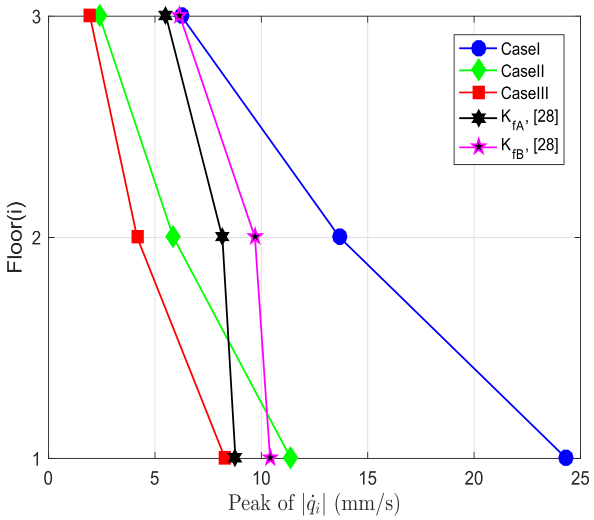

Fig. 13. Comparison results for $|\dot{q}_i|$ under the 1995 Kobe earthquakes.

$$\begin{bmatrix} \mathbf{YA}+\mathbf{A}^T\mathbf{Y}+\mathbf{Q}-\mathbf{R}+\mathbf{C}_2^T\mathbf{C}_2 & \mathbf{RW}_3 & \mathbf{0} & \mathbf{YF} & h\mathbf{A}^T\mathbf{R} \\ * & -2\mathbf{W}_3^T\mathbf{RW}_3 & \mathbf{W}_3^T\mathbf{R} & \mathbf{0} & \mathbf{0} \\ * & * & -\mathbf{Q}-\mathbf{R} & \mathbf{0} & \mathbf{0} \\ * & * & * & -\gamma^2\mathbf{I} & h\mathbf{F}^T\mathbf{R} \\ * & * & * & * & -\mathbf{R} \end{bmatrix} < 0, \tag{21}$$

$$\begin{bmatrix} \mathbf{X} & \mathbf{I} \\ * & \mathbf{Y} \end{bmatrix} > 0, \tag{22}$$

where $[\mathbf{W}_1^T, \mathbf{W}_2^T]^T$ *and* $\boldsymbol{W}_3$ *are the orthogonal complements of* $[\boldsymbol{B}^T, \boldsymbol{B}^T]^T$ *and* $\mathbf{C}_1^T$*, respectively, and*

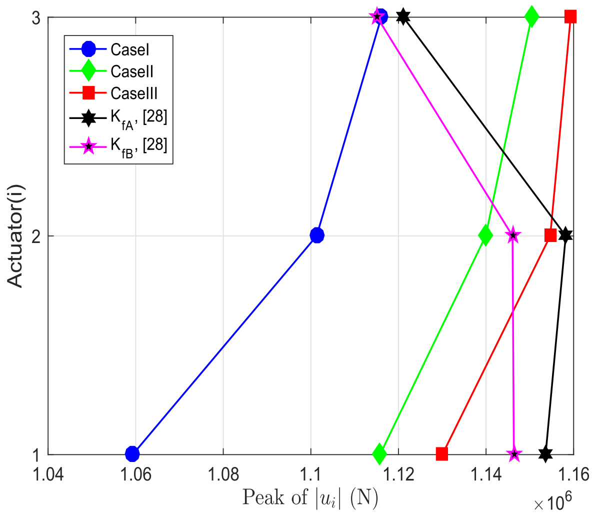

Fig. 14. Comparison results for $|u_i|$ ($i = 1,2,3$) under the 1940 El-Centro earthquakes.

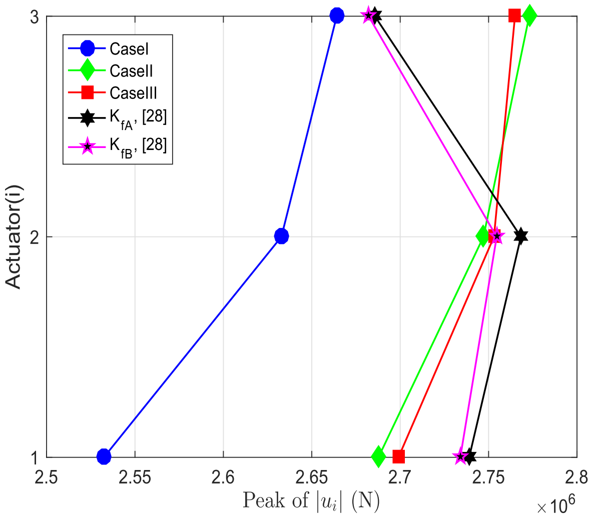

Fig. 15. Comparison results for $|u_i|$ ($i = 1,2,3$) under the 1995 Kobe earthquakes.

$$\begin{aligned}\boldsymbol{\Psi} \;=\;& \mathbf{W}_1^{\mathrm{T}}(\mathbf{AX}+\mathbf{XA}^{\mathrm{T}}+\mathbf{X}(\mathbf{Q}-\mathbf{R}+\mathbf{C}_2^{\mathrm{T}}\mathbf{C}_2)\mathbf{X})\mathbf{W}_1+\mathbf{W}_2^{\mathrm{T}}\mathbf{AXW}_1+\mathbf{W}_1^{\mathrm{T}}\mathbf{XA}^{\mathrm{T}}\mathbf{W}_2\\ &-\mathbf{h}^{-2}\mathbf{W}_2^{\mathrm{T}}\mathbf{R}^{-1}\mathbf{W}_2+\boldsymbol{\gamma}^{-2}(\mathbf{W}_1+\mathbf{W}_2)^{\mathrm{T}}\mathbf{FF}^{\mathrm{T}}(\mathbf{W}_1+\mathbf{W}_2)\end{aligned}$$

Proof. See Appendix D. □

It is clear to see that the matrix inequality (20) is still nonlinear. However, we can convert this nonlinear matrix inequality (20) into an LMI with some equality constraints. In fact, let

$$\mathbf{J} = \begin{bmatrix} \mathbf{I} & \mathbf{0} & \mathbf{0} \\ * & \mathbf{X} & \mathbf{0} \\ * & * & \mathbf{X} \end{bmatrix}$$

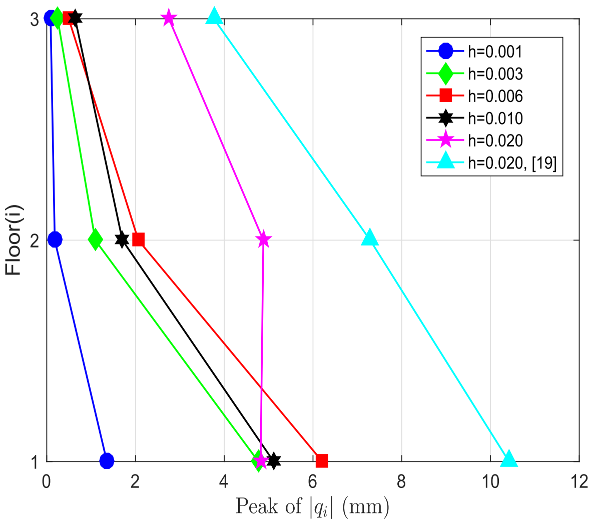

Fig. 16. Comparison of $|q_i|$ ($i = 1,2,3$) for different values of h under the 1940 El-Centro earthquakes.

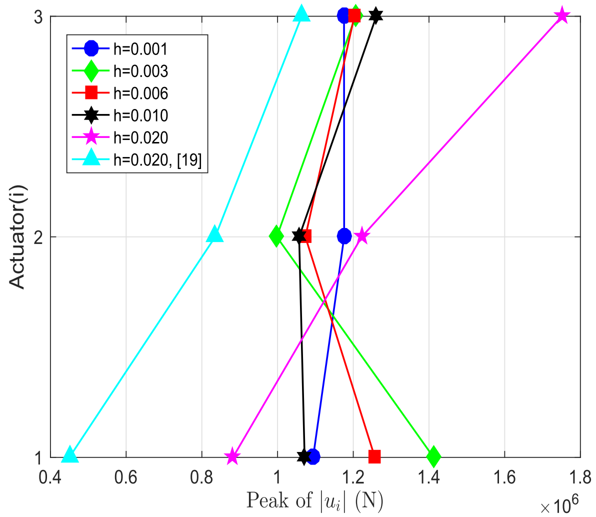

Fig. 17. Comparison of u_i ($i = 1,2,3$) for different values of h under the 1940 El-Centro earthquakes.

Then

$$\mathbf{J}^T\boldsymbol{\Gamma}\mathbf{J} = \begin{bmatrix} \boldsymbol{\Psi} & \mathbf{W}_1^T\mathbf{XRX} & \mathbf{0} \\ * & -2\mathbf{XRX} & \mathbf{XRX} \\ * & * & -\mathbf{XQX}-\mathbf{XRX} \end{bmatrix} < 0. \tag{23}$$

Now let $\mathbf{S}>0$ and $\mathbf{Z}>0$ satisfy $\mathbf{XRX} \geq \mathbf{S}$ and $\mathbf{XQX} \geq \mathbf{Z}$ Then

$$\begin{bmatrix} \mathbf{R} & \mathbf{X}^{-1} \\ \mathbf{X}^{-1} & \mathbf{S}^{-1} \end{bmatrix} \geq 0, \begin{bmatrix} \mathbf{Q} & \mathbf{X}^{-1} \\ \mathbf{X}^{-1} & \mathbf{Z}^{-1} \end{bmatrix} \geq 0.$$

Thus, the matrix inequality [23] holds if

$$\begin{bmatrix} \boldsymbol{\Psi} & \mathbf{W}_1^T\mathbf{S} & \mathbf{0} \\ * & -2\mathbf{S} & \mathbf{S} \\ * & * & -\mathbf{Z}-\mathbf{S} \end{bmatrix} < 0 \tag{24}$$

Set $\overline{\mathbf{R}} = \mathbf{R}^{-1}$, $\overline{\mathbf{Q}} = \mathbf{Q}^{-1}$, $\overline{\mathbf{Z}} = \mathbf{Z}^{-1}$, $\overline{\mathbf{S}} = \mathbf{S}^{-1}$, $\overline{\mathbf{X}} = \mathbf{X}^{-1}$. Then the nonlinear matrix inequality (20) is converted into an LMI with some equality constraints as follows.

$$\begin{bmatrix} \overline{\boldsymbol{\Psi}} & \mathbf{W}_1^T\mathbf{S} & \mathbf{0} & \mathbf{W}_1^T\mathbf{X} & \mathbf{W}_1^T\mathbf{X}\mathbf{C}_2^T \\ * & -2\mathbf{S} & \mathbf{S} & \mathbf{0} & \mathbf{0} \\ * & * & -\mathbf{Z}-\mathbf{S} & \mathbf{0} & \mathbf{0} \\ * & * & * & -\overline{Q} & \mathbf{0} \\ * & * & * & * & -\mathbf{I} \end{bmatrix} < 0 \tag{25}$$

$$\begin{bmatrix} \mathbf{R} & \overline{\mathbf{X}} \\ * & \overline{\mathbf{S}} \end{bmatrix} \geq 0, \quad \begin{bmatrix} \mathbf{Q} & \overline{\mathbf{X}} \\ * & \overline{\mathbf{Z}} \end{bmatrix} \geq 0 \tag{26}$$

$$\mathbf{R}\overline{\mathbf{R}} = \mathbf{I}, \mathbf{X}\overline{\mathbf{X}} = \mathbf{I}, \mathbf{S}\overline{\mathbf{S}} = \mathbf{I}, \mathbf{Z}\overline{\mathbf{Z}} = \mathbf{I}, \mathbf{Q}\overline{\mathbf{Q}} = \mathbf{I}, \tag{27}$$

where

$$\overline{\Psi} = \mathbf{W}_1^T \left(\mathbf{AX} + \mathbf{XA}^T - \mathbf{S}\right)\mathbf{W}_1 + \mathbf{W}_2^T\mathbf{AXW}_1 + \mathbf{W}_1^T\mathbf{XA}^T\mathbf{W}_2 - h^{-2}\mathbf{W}_2^T\overline{R}\mathbf{W}_2$$
$$+\gamma^{-2}\left(\mathbf{W}_1 + \mathbf{W}_2\right)^T\mathbf{FF}^T\left(\mathbf{W}_1 + \mathbf{W}_2\right)$$

In summary, we arrive at the following result.

Theorem 5. *For given two constants $\gamma > 0$ and $h > 0$, a desired dynamic output feedback controller can be obtained if there exist $n \times n$ real matrices $\boldsymbol{X} > 0, \overline{\boldsymbol{X}} > 0, \boldsymbol{Y} > 0, \boldsymbol{Q} > 0, \overline{\boldsymbol{Q}} > 0, \boldsymbol{R} > 0, \overline{\boldsymbol{R}} > 0, \boldsymbol{S} > 0, \overline{\boldsymbol{S}} > 0, \boldsymbol{Z} > 0$, and $\overline{\boldsymbol{Z}} > 0$, such that (21), (22), and [25–27].*

Using the cone complementary algorithm, we convert the above non-convex feasibility problem to the following nonlinear minimization problem

$$\text{Minimize}\quad Tr\left(\overline{\mathbf{Q}}\mathbf{Q} + \overline{\mathbf{R}}\mathbf{R} + \overline{\mathbf{X}}\mathbf{X} + \overline{\mathbf{Z}}\mathbf{Z} + \overline{\mathbf{S}}\mathbf{S}\right),\quad \text{Subject to}\quad (21), (22), (25), (26),\ \text{and}$$

$$\begin{bmatrix} \mathbf{R} & \mathbf{I} \\ * & \overline{\mathbf{R}} \end{bmatrix} \geq 0,\ \begin{bmatrix} \mathbf{X} & \mathbf{I} \\ * & \overline{\mathbf{X}} \end{bmatrix} \geq 0,\ \begin{bmatrix} \mathbf{Z} & \mathbf{I} \\ * & \overline{\mathbf{Z}} \end{bmatrix} \geq 0,\ \begin{bmatrix} \mathbf{S} & \mathbf{I} \\ * & \overline{\mathbf{S}} \end{bmatrix} \geq 0 \tag{28}$$

Algorithm 2 below can be used to calculate suitable $\mathcal{H}_\infty$ controllers.

Algorithm 2

1: Choose small $\gamma > 0$ and $h > 0$;

2: Find a feasible set $(\mathbf{X}^0, \mathbf{Y}^0, \overline{\mathbf{R}}^0, \overline{\mathbf{S}}^0, \mathbf{Q}^0, \mathbf{R}^0, \mathbf{S}^0, \mathbf{Z}^0, \overline{\mathbf{X}}^0, \overline{\mathbf{Q}}^0, \overline{\mathbf{Z}}^0)$ satisfying (21), (22), (25), (26) and (28). Set l = 0;

3: Solve the following optimization problem with respect to $\left(\mathbf{X}, \mathbf{Y}, \overline{\mathbf{R}}, \overline{\mathbf{S}}, \mathbf{Q}, \mathbf{R}, \mathbf{S}, \mathbf{Z}, \overline{\mathbf{X}}, \overline{\mathbf{Q}}, \overline{\mathbf{Z}}\right)$:

Minimize Tr $\left(\overline{\mathbf{X}}^l\mathbf{X} + \mathbf{X}^l\overline{\mathbf{X}} + \overline{\mathbf{R}}^l\mathbf{R} + \mathbf{R}^l\overline{\mathbf{R}} + \overline{\mathbf{Q}}^l\mathbf{Q} + \mathbf{Q}^l\overline{\mathbf{Q}} + \overline{\mathbf{Z}}^l\mathbf{Z} + \mathbf{Z}^l\overline{\mathbf{Z}} + \overline{\mathbf{S}}^l\mathbf{S} + \mathbf{S}^l\overline{\mathbf{S}}\right)$ subject to (21), (22), (25), (26) and (28). Set $\overline{\mathbf{Z}}^{l+1} = \overline{\mathbf{Z}}$, $\mathbf{X}^{l+1} = \mathbf{X}$, $\mathbf{X}^{l+1} = \mathbf{X}$, $\mathbf{Q}^{l+1} = \mathbf{Q}$, $\mathbf{R}^{l+1} = \mathbf{R}$, $\mathbf{Z}^{l+1} = \mathbf{Z}$, $\mathbf{S}^{l+1} = \mathbf{S}$, $\overline{\mathbf{X}}^{l+1} = \overline{\mathbf{X}}$, $\overline{\mathbf{Q}}^{l+1} = \overline{\mathbf{Q}}$, $\overline{\mathbf{R}}^{l+1} = \overline{\mathbf{R}}$, $\overline{\mathbf{S}}^{l+1} = \overline{\mathbf{S}}$;

3: Solve the following optimization problem with respect to $\left(\mathbf{X}, \mathbf{Y}, \overline{\mathbf{R}}, \overline{\mathbf{S}}, \mathbf{Q}, \mathbf{R}, \mathbf{S}, \mathbf{Z}, \overline{\mathbf{X}}, \overline{\mathbf{Q}}, \overline{\mathbf{Z}}\right)$:

Minimize Tr $\left(\overline{\mathbf{X}}^l\mathbf{X} + \mathbf{X}^l\overline{\mathbf{X}} + \overline{\mathbf{R}}^l\mathbf{R} + \mathbf{R}^l\overline{\mathbf{R}} + \overline{\mathbf{Q}}^l\mathbf{Q} + \mathbf{Q}^l\overline{\mathbf{Q}} + \overline{\mathbf{Z}}^l\mathbf{Z} + \mathbf{Z}^l\overline{\mathbf{Z}} + \overline{\mathbf{S}}^l\mathbf{S} + \mathbf{S}^l\overline{\mathbf{S}}\right)$ subject to (21), (22), (25), (26) and (28). Set $\overline{\mathbf{Z}}^{l+1} = \overline{\mathbf{Z}}$, $\mathbf{X}^{l+1} = \mathbf{X}$, $\mathbf{X}^{l+1} = \mathbf{X}$, $\mathbf{Q}^{l+1} = \mathbf{Q}$, $\mathbf{R}^{l+1} = \mathbf{R}$, $\mathbf{Z}^{l+1} = \mathbf{Z}$, $\mathbf{S}^{l+1} = \mathbf{S}$, $\overline{\mathbf{X}}^{l+1} = \overline{\mathbf{X}}$, $\overline{\mathbf{Q}}^{l+1} = \overline{\mathbf{Q}}$, $\overline{\mathbf{R}}^{l+1} = \overline{\mathbf{R}}$, $\overline{\mathbf{S}}^{l+1} = \overline{\mathbf{S}}$;

4: If $|\text{Tr}(\overline{\mathbf{X}}^l\mathbf{X} + \mathbf{X}^l\overline{\mathbf{X}} + \overline{\mathbf{R}}^l\mathbf{R} + \mathbf{R}^l\overline{\mathbf{R}} + \overline{\mathbf{Q}}^l\mathbf{Q} + \mathbf{Q}^l\overline{\mathbf{Q}} + \overline{\mathbf{Z}}^l\mathbf{Z} + \mathbf{Z}^l\overline{\mathbf{Z}} + \overline{\mathbf{S}}^l\mathbf{S} + \mathbf{S}^l\overline{\mathbf{S}}) - 60| < \varepsilon$, where $\varepsilon > 0$ is sufficiently small, is satisfied, then go to Step 5. Otherwise, set $l = l + 1$ and go to Step 3. If the above condition is violated within a number of iterations, then exit;

5: Compute by the singular value decomposition $\mathbf{M} \in \mathbb{R}^{n\times n}$ and $\mathbf{N} \in \mathbb{R}^{n\times n}$ such that $\mathbf{MN}^T = \mathbf{I} - \mathbf{XY}$;

6: Determine the matrix $\mathbf{P}$ by

$$\mathbf{P} = \begin{bmatrix} \mathbf{Y} & \mathbf{I} \\ \mathbf{N}^T & \mathbf{0} \end{bmatrix}\begin{bmatrix} \mathbf{I} & \mathbf{X} \\ \mathbf{0} & \mathbf{M}^T \end{bmatrix}^{-1};$$

7: With the obtained $\mathbf{P}$, $\mathbf{Q}$, and $\mathbf{R}$, solve the controller gain $\mathbf{K}$ from (19);

8: If there is no feasible solution to (19), change the values of γ and h, and go to step 2.

---

4. Simulation study

In this section a three-storey building model [28] is studied, where the masses, damping and stiffness coefficients for each storey are given by $m_i = 345.6$ ton, $c_i = 2973$ kNs/m, and $k_i = 3.404 \times 10^5$ kN/m, $i = 1, 2, 3$, respectively. Three actuators, each of them for a storey, are located in the building, which leads to $\mathbf{H}_0 = \mathbf{I}$. It is also assumed that the velocity sensors are the only available outputs for measurement, i.e. $\mathbf{C}_1 = [\mathbf{0}_{3\times3}, \mathbf{I}]$.

For practice, the 1940 El-Centro and 1995 Kobe earthquakes real-data, shown in Figs. 3 and 4, are utilized for the input disturbance $w(t)$ introduced in (2). When the earthquake force is applied to the building model without a controller, the peak of absolute relative drift for the first storey is about 20 mm and 60 mm for the El-Centro and Kobe earthquakes, respectively. Since this building is a short one, as mentioned in Remark 1, the peaks of absolute relative drift of second and third storeys are smaller than the first storey. Therefore, we should emphasize the performance index (4) on the first floor by selecting a proper matrix $\mathbf{C}_2$. In the following, the objective is to design suitable dynamic output feedback $\mathcal{H}_\infty$ controllers under two schemes.

4.1. Continuous-signal-based dynamic output feedback $\mathcal{H}_\infty$ control design

In this subsection, suppose that the continuous output measurements are available for control design. Then, we use Algorithm 1 to design a dynamic output feedback controller. In the sequel, it is shown that choosing a proper matrix $\mathbf{C}_2$ can improve

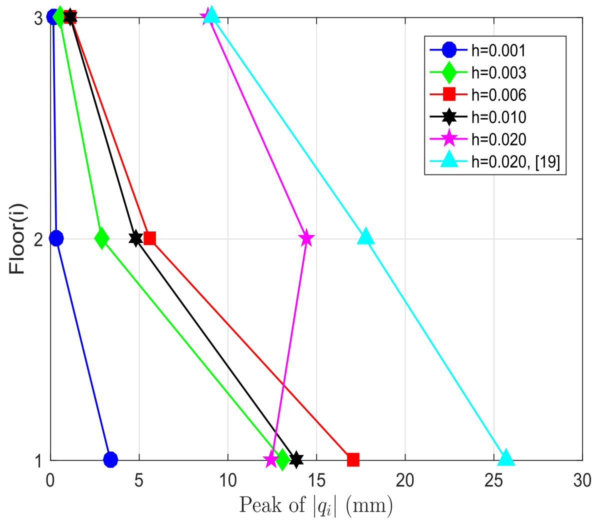

Fig. 18. Comparison of $|q_i|$ $(i = 1,2,3)$ for different values of h under the 1995 Kobe earthquakes.

the control performance in the sense of the peaks of the absolute values of relative drifts and their derivatives in each storey, i.e. $|q_i|$ and $|\dot{q}_i| \quad (i = 1,2,3)$. For this purpose, we consider three cases of $\mathbf{C}_2$.

Case I: $\mathbf{C}_2 = [\mathbf{I}, \quad \mathbf{0}_{3\times3}]$. Under Case I, we aim to control the relative drifts for each storey with equal importance degree. Applying Theorem 2, the minimum $\mathcal{H}_\infty$ performance γ can be obtained as $\gamma_{\min} = 0.02$. The corresponding controller can be solved out by Algorithm 1, whose gains are given as follows

$$
\mathbf{A}_c = 10^7 \times \begin{bmatrix} -0.3919 & 0.0016 & -0.0020 & 0 & 0 & 0.0019 \\ 0.0018 & -0.3898 & -0.0039 & 0 & 0.0019 & 0 \\ -0.0017 & -0.0039 & -0.3887 & -0.0018 & 0 & 0 \\ -0.0062 & -0.0135 & -1.5742 & -0.0074 & 0.0001 & 0 \\ -0.0072 & 1.5974 & 0.0175 & 0.0001 & -0.0077 & 0 \\ 1.6030 & -0.0068 & 0.0086 & 0 & 0 & -0.0078 \end{bmatrix}
$$

$$
B_c = 10^5 \times \begin{bmatrix} -0.2277 & 0.5170 & -0.4155 \\ -0.4128 & 0.2244 & 0.5157 \\ 0.5011 & 0.4202 & 0.2371 \\ 2.0328 & 1.6997 & 0.9579 \\ 1.6895 & -0.9217 & -2.1139 \\ 0.9306 & -2.1150 & 1.6996 \end{bmatrix}
$$

$$
C_c = 10^8 \times \begin{bmatrix} 0.0227 & 0.0173 & 0.0001 & -1.4156 & -1.8987 & -1.0920 \\ -0.0283 & 0.0077 & -0.0006 & -2.5004 & -0.8723 & 1.3365 \\ 0.0126 & -0.0139 & -0.0010 & -3.1179 & 1.4494 & -0.6092 \end{bmatrix}
$$

$$
D_c = 10^8 \times \begin{bmatrix} -1.6687 & 1.4012 & 0.0364 \\ -0.2593 & -1.6240 & 1.4046 \\ -0.2194 & -0.2557 & -1.6603 \end{bmatrix}.
$$

Under the obtained controller, the peak of absolute relative drift of the first floor is 1.1 mm and 2.8 mm for El-Centro and Kobe earthquakes, respectively, which is about twenty times smaller than those when no controller is imposed on the building. Notice that the derivatives of the relative drifts are not considered under Case I.

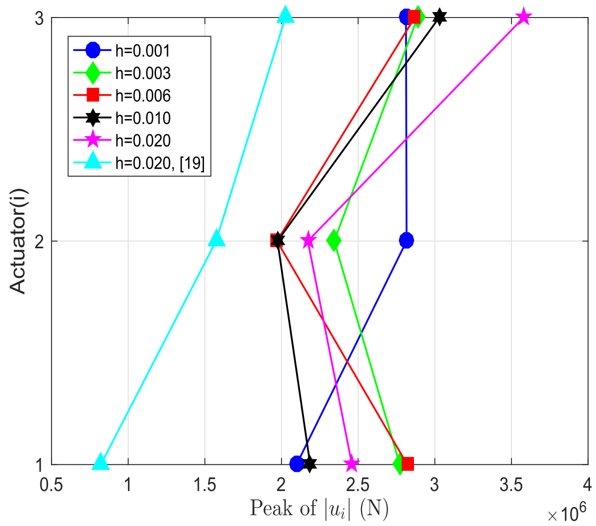

Fig. 19. Comparison of u_i ($i = 1,2,3$) for different values of h under the 1995 Kobe earthquakes.

Case II: $C_2 = I$. In this case, both the relative drifts and their derivatives are taken to be the control objective with identical degree of importance. Applying Theorem 2 gives the minimum $\mathcal{H}_\infty$ performance level $\gamma_{\min} = 0.02$, and the corresponding controller gains can be derived using Algorithm 1, which are omitted for space saving. Under this controller, the peak of absolute relative drift of the first floor is decreased to 0.5 mm and 1.1 mm for El-Centro and Kobe earthquakes, respectively. Thus, one can see that taking the derivatives of the relative drifts into account can result in some better control performance if compared with Case I.

Case III: $C_2 = \mathrm{diag}\{3,1,1,3,1,1\}$. From the analysis in Cases I and II, it is seen that the peak of relative drift for the first floor is about two and three times bigger than the second and third floors, respectively, for both earthquakes. Thus, the first floor is important for this short building. In order to enhance the relative drift of the first floor and its derivative, we increase the value of corresponding gain of $\mathbf{x}_1(t)\,(=\mathbf{q}_1(t))$ and $\mathbf{x}_4(t)\,(=\dot{\mathbf{q}}_1(t))$ in the matrix $\mathbf{C}_2$ from 1 to 3 such that Algorithm 1 is solvable. Then, employ Theorem 2 to get the minimum $\gamma = 0.03$ and an $\mathcal{H}_\infty$ controller of form (8) whose gains are omitted. Under the controller, the responses of relative drifts of the first floor are depicted in Fig. 5, from which the peak of absolute relative drift of the first floor are decreased to 0.4 mm and 0.8 mm for El-Centro and Kobe earthquakes, respectively. Thus, tuning the matrix $\mathbf{C}_2$ indeed can help improve the control performance of the building. Moreover, both closed-loop and open-loop responses of relative velocity drifts and relative acceleration of the first floor for El-Centro and Kobe earthquakes are plotted in Figs. 6–9, from which it is shown that the relative velocity drifts and relative accelerations are significantly decreased under the proposed

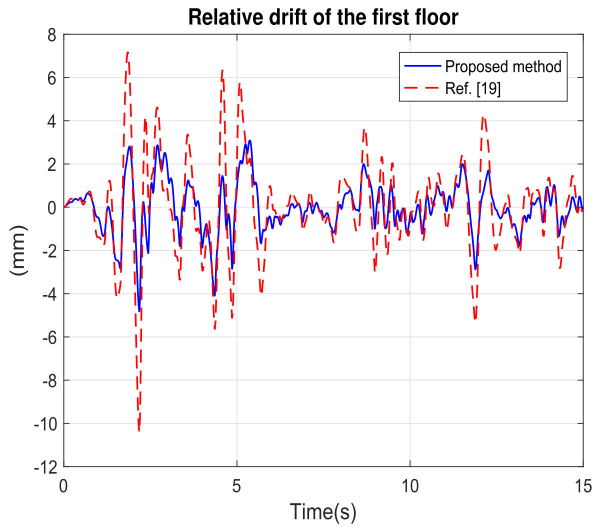

Fig. 20. The responses of relative drift of the first floor to 1940 El-Centro earthquakes.

controller.

In order to further demonstrate the effectiveness of the above results, we compare with the method proposed in Ref. [28], where state feedback control is considered with the control gains $\mathbf{K}_{fA}$ and $\mathbf{K}_{fB}$ being given in Ref. [28]. Under the controllers obtained in this paper and [28], the peaks of absolute value of the relative drifts and their derivatives for three floors are shown in Figs. 10–13 for El-Centro and Kobe earthquakes, respectively. Besides, the maximum absolute values of control forces for each storey are also depicted in Figs. 14 and 15. From Figs. 10–15, one can see that

- The controller designed in Case III can produce some smaller peaks of absolute values of relative drifts of all storeys than those in Ref. [28]; and
- The peaks of absolute values of control signals, i.e. $|u_i|$, in Case III are almost equal to those in Ref. [28] except for the third floor, which means that the same size of actuators is needed for the first and the second floors.

Overall, the controller under Case III achieves better control performance in controlling the peaks of absolute values of relative drifts of all storeys if compared with the method in Ref. [28], while the size of actuators needed and the energy consumption of the controllers are almost the same.

4.2. Sampled-data-based dynamic output feedback controller design

This subsection aims at designing dynamic output feedback controllers for the building in the case where the output signals are sampled in the digital form. Set $\gamma = 0.1$ and $\mathbf{C}_2 = \mathrm{diag}\{3,1,1,3,1,1\}$. For different sampling periods of $h \in \{1\text{ms}, 3\text{ms}, 6\text{ms}, 10\text{ms}, 20\text{ms}\}$, by Algorithm 2, it is found that the $\mathcal{H}_\infty$ control problem is solvable and corresponding $\mathcal{H}_\infty$ controllers can be designed. Under these controllers, the peaks of absolute relative drift and the peaks of control force of each storey are illustrated in Figs. 16–19 for the El-Centro and Kobe earthquakes, respectively. From these figures, a smaller sampling period is expected to achieve better control performance, which is reasonable from the practical point of view.

For comparison with the method in Ref. [19], we design the $\mathcal{H}_\infty$ controller of form (16) for $h = 0.02$ms using Algorithm 2, and the corresponding controller gains are given by

$$\mathbf{A}_c = \begin{bmatrix} -17.249 & -4.9196 & 16.316 & 0.0031 & 2.3301 & -1.3134 \\ 4.0104 & -13.330 & -8.3408 & -7.8418 & 13.592 & -16.590 \\ 2.1380 & -0.6848 & -22.768 & -15.622 & -32.293 & 27.396 \\ -23.177 & 1.8515 & 20.446 & -1.7450 & -18.072 & 19.601 \\ 36.300 & -24.405 & -77.541 & -42.048 & -23.193 & 6.7753 \\ 17183 & -9432.1 & -28012 & -12676 & 3117.5 & -8373.7 \end{bmatrix}$$

$$B_c = \begin{bmatrix} -0.0147 & 0.0057 & 0.0427 \\ 1.0432 & 1.1277 & 0.43579 \\ -1.1996 & -1.3965 & -0.6142 \\ -1.2237 & -1.3983 & -1.2981 \\ 2.4925 & 2.3023 & 1.2999 \\ 1097.6 & 1011 & 623.97 \end{bmatrix}$$

$$C_c = 10^8 \times \begin{bmatrix} -3.5511 & 2.2502 & 3.4881 & 1.1727 & 2.7738 & -2.2110 \\ 5.3760 & 0.9860 & 1.1460 & 0.6024 & 0.6047 & -0.2397 \\ -2.1858 & -2.6712 & -2.4091 & -0.3038 & -0.3418 & 0.2950 \end{bmatrix}$$

$$D_c = 10^7 \times \begin{bmatrix} 0.2497 & 0.4971 & 0.3751 \\ -0.9488 & -0.8245 & -0.3394 \\ -1.1209 & -1.0709 & -0.7656 \end{bmatrix}$$

Associated with the above controller and that in Ref. [19], the peaks of absolute relative drifts for each storey are plotted in Figs. 16–19, and the relative drifts of the first floor are given in Figs. 20 and 21 for El-Centro and Kobe earthquakes, respectively. Based on these figures, the proposed method can provide better control performance in controlling the peak of absolute relative drifts for each storey.

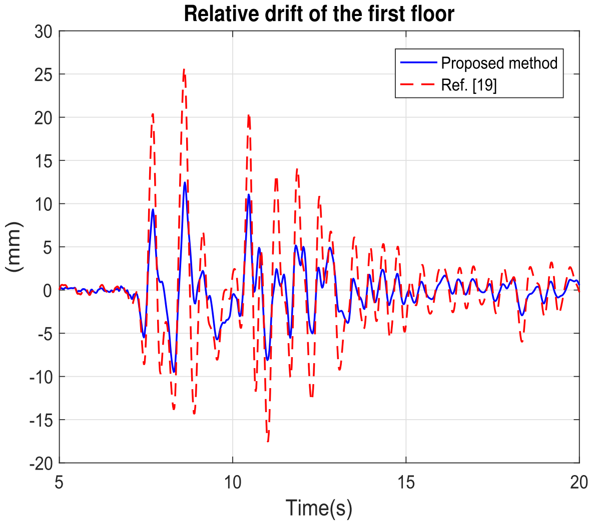

Fig. 21. The responses of relative drift of the first floor to 1995 Kobe earthquakes.

5. Conclusion

The problem of dynamic output feedback control for a seismic-excited building has been investigated. Two kinds of schemes have been devised depending on whether the system measurements are sampled or not. The Lyapunov stability theory has been employed to formulate some criteria on the existence of such controllers. The cone complementary algorithm has been used to design suitable $\mathcal{H}_\infty$ controllers. In the simulation study, a three-storey building model has finally given to illustrate the advantages of the proposed results, where two earthquakes real-data was utilized as the input disturbance imposed on the building model. It has been shown that the proposed controllers can reduce the relative drifts of the floors significantly. Moreover, it has been shown that choosing a proper matrix $\mathbf{C}_2$ can improve the control performance in the sense of the peaks of the absolute values of relative drifts and their derivatives in each storey. Compared with some existing methods, the proposed method can not only achieve better performance but also require less control effort and less energy in a couple of floors.

Appendix A. Proof of Theorem 1

Choose a Lyapunov function as

$$V(t) = \xi^T(t)\mathbf{P}\xi(t) \tag{29}$$

Calculating $\dot{V}(t)$ yields

$$\dot{V}(t) = 2\xi^T(t)\mathbf{P}\dot{\xi}(t) = 2\xi^T(t)\mathbf{P}\left(\left(\mathbf{A}_0 + \mathbf{HKL}\right)\xi(t) + \mathbf{E}^T\mathbf{F}\mathbf{w}(t)\right). \tag{30}$$

From Eqs. (4) and (30), one has

$$\dot{V}(t) + \mathbf{z}^T(t)\mathbf{z}(t) - \gamma^2\mathbf{w}^T(t)\mathbf{w}(t) \le \zeta^T(t)\mathbf{\Phi}\zeta(t), \tag{31}$$

where $\zeta(t) = [\xi^T(t),\mathbf{w}^T(t)]^T$ and $\mathbf{\Phi}$ is defined in (11). If condition (11) is satisfied, i.e. $\mathbf{\Phi} < 0$, then from Eq. (31), one obtains

$$\dot{V}(t) + \mathbf{z}^T(t)\mathbf{z}(t) - \gamma^2\mathbf{w}^T(t)\mathbf{w}(t) < 0. \tag{32}$$

A zero initial condition gives

$$\int_0^\infty \left[\mathbf{z}^T(t)\mathbf{z}(t) - \gamma^2\mathbf{w}^T(t)\mathbf{w}(t)\right] dt \le 0, \tag{33}$$

which means that the inequality (4) is satisfied. □

Appendix B. Proof of Theorem 2

For eliminating the matrix **K** from (11), we use Lemma 1. The matrix $\mathbf{\Phi}$ in (11) can be rewritten as

$$\mathbf{\Phi} = \mathbf{\Phi}_0 + \mathbf{\Sigma\Pi K\Theta}^T + \mathbf{\Theta K}^T\mathbf{\Pi}^T\mathbf{\Sigma}^T < 0, \tag{34}$$

where $\mathbf{\Sigma} = \mathrm{diag}\{\mathbf{P},\mathbf{I}\}$, $\mathbf{\Pi} = [\mathbf{H}^T, \mathbf{0}]^T$, $\mathbf{\Theta} = [\mathbf{L}, \mathbf{0}]^T$, and

$$\mathbf{\Phi}_0 = \begin{bmatrix} \mathbf{PA}_0 + \mathbf{A}_0^T\mathbf{P} + \mathbf{E}^T\mathbf{C}_2^T\mathbf{C}_2\mathbf{E} & \mathbf{PE}^T\mathbf{F} \\ * & -\gamma^2\mathbf{I} \end{bmatrix} < 0$$

From Lemma 1, there exists $\mathbf{K}$ such that (34) if and only if

$$\mathbf{\Pi}_{\perp}^{T}\mathbf{\Sigma}^{-1}\mathbf{\Phi}_0\mathbf{\Sigma}^{-1}\mathbf{\Pi}_{\perp} < 0, \tag{35}$$

$$\mathbf{\Theta}_{\perp}^{T}\mathbf{\Phi}_0\mathbf{\Theta}_{\perp} < 0, \tag{36}$$

where $\mathbf{\Pi}_{\perp}$ and $\mathbf{\Theta}_{\perp}$ are the orthogonal complements of $\mathbf{\Pi}$ and $\mathbf{\Theta}$, respectively. To simplify the expressions in (35) and (36), we partition $\mathbf{P}$ and $\mathbf{P}^{-1}$ as

$$\mathbf{P} = \begin{bmatrix} \mathbf{Y} & \mathbf{N} \\ \mathbf{N}^T & \# \end{bmatrix}, \quad \mathbf{P}^{-1} = \begin{bmatrix} \mathbf{X} & \mathbf{M} \\ \mathbf{M}^T & \# \end{bmatrix} \tag{37}$$

where $\mathbf{X}, \mathbf{Y}, \mathbf{N}, \mathbf{M} \in \mathbb{R}^{n\times n}$ and # denotes an irrelevant matrix. Let $\mathbf{W}_1$ and $\mathbf{W}_2$ be the orthogonal complements of $\mathbf{B}$ and $\mathbf{C}_1^T$, respectively. Then,

$$\mathbf{\Pi}_{\perp} = \begin{bmatrix} \mathbf{W}_1 & \mathbf{0} \\ \mathbf{0} & \mathbf{0} \\ \mathbf{0} & \mathbf{I} \end{bmatrix}, \quad \mathbf{\Theta}_{\perp} = \begin{bmatrix} \mathbf{W}_2 & \mathbf{0} \\ \mathbf{0} & \mathbf{0} \\ \mathbf{0} & \mathbf{I} \end{bmatrix}.$$

Consequently, the inequality (35) becomes

$$\begin{bmatrix} \mathbf{W}_1^T\left(\mathbf{AX} + \mathbf{XA}^T + \mathbf{XC}_2^T\mathbf{C}_2\mathbf{X}\right)\mathbf{W}_1 & \mathbf{W}_1^T\mathbf{F} \\ * & -\gamma^2\mathbf{I} \end{bmatrix} < 0, \tag{38}$$

which is equivalent to

$$\mathbf{W}_1^T\left(\mathbf{AX} + \mathbf{XA}^T + \mathbf{XC}_2^T\mathbf{C}_2\mathbf{X}\right)\mathbf{W}_1 + \gamma^{-2}\mathbf{W}_1^T\mathbf{FF}^T\mathbf{W}_1 < 0. \tag{39}$$

The Schur complement follows that the inequality (39) is equivalent to (12). Similarly, the inequality (36) is equivalent to (13). Moreover, from Lemma 2, there exists a $\mathbf{P} > 0$ satisfying (37) if and only if $\mathbf{X} - \mathbf{Y} \geq 0$, which is equivalent to (14). □

Appendix C. Proof of Theorem 3

Take a Lyapunov-Krasovskii functional as

$$V(t) = \xi^T(t)\mathbf{P}\xi(t) + \int_{t-h}^{t}\xi^T(s)\mathbf{E}^T\mathbf{QE}\xi(s)\,ds + h\int_{-h}^{0}\int_{t+\theta}^{t}\dot{\xi}^T(s)\mathbf{E}^T\mathbf{RE}\dot{\xi}(s)\,dsd\theta. \tag{40}$$

The time-derivative of $V(t)$ gives

$$\begin{aligned} \dot{V}(t) = {}& 2\xi^T(t)\mathbf{P}\dot{\xi}(t) + \xi^T(t)\mathbf{E}^T\mathbf{QE}\xi(t) - \xi^T(t-h)\mathbf{E}^T\mathbf{QE}\xi(t-h) + h^2\dot{\xi}^T(t)\mathbf{E}^T\mathbf{RE}\dot{\xi}(t) \\ & -h\int_{t-h}^{t-d(t)}\dot{\xi}^T(s)\mathbf{E}^T\mathbf{RE}\dot{\xi}(s)\,ds - h\int_{t-d(t)}^{t}\dot{\xi}^T(s)\mathbf{E}^T\mathbf{RE}\dot{\xi}(s)\,ds. \end{aligned} \tag{41}$$

From (4), (18), (30), and together with the Jensen inequality, one has

$$\dot{V}(t) + \mathbf{z}^T(t)\mathbf{z}(t) - \gamma^2\mathbf{w}^T(t)\mathbf{w}(t) \leq \zeta^T(t)\widetilde{\mathbf{\Phi}}\zeta(t), \tag{42}$$

where $\zeta(t) = \begin{bmatrix} \xi^T(t) & \mathbf{E}\xi^T(t-d(t)) & \mathbf{E}\xi^T(t-h) & \mathbf{w}^T(t) \end{bmatrix}^T$, and

$$\begin{cases} \widetilde{\Phi} = \begin{bmatrix} \Xi_1 & \Xi_2 & \mathbf{0} & \mathbf{PE}^T\mathbf{F} \\ * & -2\mathbf{R} & \mathbf{R} & \mathbf{0} \\ * & * & -\mathbf{Q}-\mathbf{R} & \mathbf{0} \\ * & * & * & -\gamma^2\mathbf{I} \end{bmatrix} + \mathbf{UR}^{-1}\mathbf{U}^T < 0, \\ \mathbf{U} = \begin{bmatrix} h\left(\mathbf{A}_0 + \mathbf{HKL}_1\right)^T\mathbf{E}^T\mathbf{R} \\ h\left(\mathbf{HKL}_2\right)^T\mathbf{E}^T\mathbf{R} \\ \mathbf{0} \\ h\mathbf{F}^T\mathbf{R} \end{bmatrix}, \end{cases} \tag{43}$$

which is equivalent to (19). The rest of proof is similar to Theorem 1. □

Appendix D. Proof of Theorem 4

For eliminating the design matrix $\mathbf{K}$ from Eq. (19), we use Lemma 1. Rewrite the matrix $\overline{\mathbf{\Phi}}$ in (19) to get

$$\overline{\mathbf{\Phi}} = \overline{\mathbf{\Phi}}_0 + \mathbf{\Sigma\Pi K \Theta}^T + \mathbf{\Theta K}^T\mathbf{\Pi}^T\mathbf{\Sigma}^T < 0, \tag{44}$$

where $\mathbf{\Sigma} = \mathrm{diag}\{\mathbf{P}, \mathbf{I}, \mathbf{I}, \mathbf{I}, \mathbf{I}\}$, $\mathbf{\Pi} = [\mathbf{H}^T, \mathbf{0}, \mathbf{0}, \mathbf{0}, h\mathbf{H}^T\mathbf{E}^T]^T$, $\mathbf{\Theta} = [\mathbf{L}_1, \mathbf{L}_2, \mathbf{0}, \mathbf{0}, \mathbf{0}]^T$, and

$$\overline{\Phi}_0 = \begin{bmatrix} \overline{\Xi}_1 & \mathbf{E}^T\mathbf{R} & \mathbf{0} & \mathbf{PE}^T\mathbf{F} & h\mathbf{A}_0^T\mathbf{E}^T\mathbf{R} \\ * & -2\mathbf{R} & \mathbf{R} & \mathbf{0} & \mathbf{0} \\ * & * & -\mathbf{Q}-\mathbf{R} & \mathbf{0} & \mathbf{0} \\ * & * & * & -\gamma^2\mathbf{I} & h\mathbf{F}^T\mathbf{R} \\ * & * & * & * & -\mathbf{R} \end{bmatrix} < 0,$$

$$\overline{\Xi}_1 = \mathbf{PA}_0 + \mathbf{A}_0^T\mathbf{P} + \mathbf{E}^T\mathbf{QE} - \mathbf{E}^T\mathbf{RE} + \mathbf{E}^T\mathbf{C}_2^T\mathbf{C}_2\mathbf{E}.$$

Based on Lemma 1, the matrix $\mathbf{K}$, satisfying Eq. (44), exists if and only if

$$\mathbf{\Pi}_\perp^T\mathbf{\Sigma}^{-1}\overline{\Phi}_0\mathbf{\Sigma}^{-1}\mathbf{\Pi}_\perp < 0, \tag{45}$$

$$\mathbf{\Theta}_\perp^T\overline{\Phi}_0\mathbf{\Theta}_\perp < 0, \tag{46}$$

where $\mathbf{\Pi}_\perp$ and $\mathbf{\Theta}_\perp$ are orthogonal complements of $\mathbf{\Pi}$ and $\mathbf{\Theta}$, as follows:

$$\mathbf{\Pi}_\perp = \begin{bmatrix} \mathbf{W}_1 & \mathbf{0} & \mathbf{0} & \mathbf{0} \\ \mathbf{0} & \mathbf{0} & \mathbf{0} & \mathbf{0} \\ \mathbf{0} & \mathbf{I} & \mathbf{0} & \mathbf{0} \\ \mathbf{0} & \mathbf{0} & \mathbf{I} & \mathbf{0} \\ \mathbf{0} & \mathbf{0} & \mathbf{0} & \mathbf{I} \\ \frac{1}{h}\mathbf{W}_2 & \mathbf{0} & \mathbf{0} & \mathbf{0} \end{bmatrix}, \quad \mathbf{\Theta}_\perp = \begin{bmatrix} \mathbf{I} & \mathbf{0} & \mathbf{0} & \mathbf{0} & \mathbf{0} \\ \mathbf{0} & \mathbf{0} & \mathbf{0} & \mathbf{0} & \mathbf{0} \\ \mathbf{0} & \mathbf{W}_3 & \mathbf{0} & \mathbf{0} & \mathbf{0} \\ \mathbf{0} & \mathbf{0} & \mathbf{I} & \mathbf{0} & \mathbf{0} \\ \mathbf{0} & \mathbf{0} & \mathbf{0} & \mathbf{I} & \mathbf{0} \\ \mathbf{0} & \mathbf{0} & \mathbf{0} & \mathbf{0} & \mathbf{I} \end{bmatrix}.$$

The rest of proof is similar to Theorem 3. □

References

[1] T. Soong, M. Costantinou, Passive and Active Structural Vibration Control in Civil Engineering, Springer, 2014. https://books.google.com/books?isbn=3709130123.

[2] T.Sakr, Vibration control of buildings by using partial floor loads as multiple tuned mass dampers,, HBRC J., 13 (2) (2017) 133–144, http://dx.doi.org/10.1016/j.hbrcj.2015.04.004.

[3] A.-P. Wang, Y.-H. Lin, Vibration control of a tall building subjected to earthquake excitation, J. Sound. Vib. 299 (4) (2007) 757–773, http://dx.doi.org/10.1016/j.jsv.2006.07.016.

[4] B.-L. Zhang, Q.-L. Han, X.-M. Zhang, Recent advances in vibration control of offshore platforms, Nonlinear Dyn. 89 (2) (2017) 755–771, http://dx.doi.org/10.1007/s11071-017-3503-4.

[5] D.-H. Yang, J.-H. Shin, H. Lee, S.-K. Kim, M.-K. Kwak, Active vibration control of structure by active mass damper and multi-modal negative acceleration feedback control algorithm, J. Sound. Vib. 392 (2017) 18–30, http://dx.doi.org/10.1016/j.jsv.2016.12.036.

[6] A. Aly, Vibration control of buildings using magnetorheological damper: a new control algorithm, J. Eng. 2013 (2013) 1–10, http://dx.doi.org/10.1155/2013/596078.

[7] M. Askari, J. Li, B. Samali, Semi-active lqg control of seismically excited nonlinear buildings using optimal takagi-sugeno inverse model of mr dampers, Procedia Eng. 14 (2011) 1013–1020, http://dx.doi.org/10.1016/j.proeng.2011.07.127.

[8] H. Garrido, O. Curadelli, D. Ambrosini, Semi-active friction tendons for vibration control of space structures, J. Sound. Vib. 333 (22) (2014) 5657–5679, http://dx.doi.org/10.1016/j.jsv.2014.06.018.

[9] S. Korkmaz, A review of active structural control: challenges for engineering informatics, Comput. Struct. 89 (23) (2011) 2113–2132, http://dx.doi.org/10.1016/j.compstruc.2011.07.010.

[10] T. Soong, Active structural control: theory and practice, J. Eng. Mech. 118 (6) (1992) 1282–1285, http://dx.doi.org/10.1061/(ASCE)0733-9399(1992)118:6(1282).

[11] Y. Ikeda, Active and semi-active vibration control of buildings in Japan – practical applications and verification, Struct. Control Health Monit. 16 (7–8) (2009) 703–723, http://dx.doi.org/10.1002/stc.315.

[12] U. Aldemir, A simple active control algorithm for earthquake excited structures, Comput. Aid. Civ. Infrastruct. Eng. 25 (3) (2010) 218–225, http://dx.doi.org/10.1111/j.1467-8667.2009.00629.x.

[13] S. Pourzeynali, H. Lavasani, A. Modarayi, Active control of high rise building structures using fuzzy logic and genetic algorithms, Eng. Struct. 29 (3) (2007) 346–357, http://dx.doi.org/10.1016/j.engstruct.2006.04.015.

[14] B. Spencer Jr., , S. Nagarajaiah, State of the art of structural control, J. Struct. Eng. 129 (7) (2003) 845–856, http://dx.doi.org/10.1061/(ASCE)0733-9445(2003)129:7(845).

[15] M. Mahmoud, M. Zribi, Y. Soh, Optimal control of seismically-excited building structures, Comput. Struct. 74 (5) (2000) 521–533, http://dx.doi.org/10.1016/S0045-7949(99)\ignorespaces00054–1.

[16] G. Mei, A. Kareem, J. Kantor, Model predictive control of structures under earthquakes using acceleration feedback, J. Eng. Mech. 128 (5) (2002) 574–585, http://dx.doi.org/10.1061/(ASCE)0733-9399(2002)128:5(574).

[17] S.-G. Wang, Robust active control for uncertain structural systems with acceleration sensors, Struct. Control Health Monit. 10 (1) (2003) 59–76, http://dx.doi.org/10.1002/stc.17.
[18] J.-C. Wu, H.-H. Chih, C.-H. Chen, A robust control method for seismic protection of civil frame building, J. Sound. Vib. 294 (1) (2006) 314–328, http://dx.doi.org/10.1016/j.jsv.2005.11.019.
[19] H. Du, N. Zhang, B. Samali, F. Naghdy, Robust sampled-data control of structures subject to parameter uncertainties and actuator saturation, Eng. Struct. 36 (2012) 39–48, http://dx.doi.org/10.1016/j.engstruct.2011.11.024.
[20] A. Madan, Vibration control of building structures using self-organizing and self-learning neural networks, J. Sound. Vib. 287 (4) (2005) 759–784, http://dx.doi.org/10.1016/j.jsv.2004.11.031.
[21] H. Cho, M. Fadali, M. Saiidi, K. Lee, Neural network active control of structures with earthquake excitation, Int. J. Control Autom. Syst. 2 (2005) 202–210. http://ijcas.org/admin/paper/files/IJCAS_v3_n2_pp.202-210.pdf.
[22] P. Alvarez, B. McElwain, L. Thesing, S. Edalath, A. Kukreti, K. Cohen, PD and fuzzy logic control for earthquake resilient structures, Comput. Appl. Eng. Educ. 22 (1) (2014) 142–152, http://dx.doi.org/10.1002/cae.20540.
[23] R. Guclu, Sliding mode and pid control of a structural system against earthquake, Math. Comput. Model 44 (1) (2006) 210–217, http://dx.doi.org/10.1016/j.mcm.2006.01.014.
[24] S. Thenozhi, W. Yu, Stability analysis of active vibration control of building structures using PD/PID control, Eng. Struct. 81 (2014) 208–218, http://dx.doi.org/10.1016/j.engstruct.2014.09.042.
[25] X.-M. Zhang, Q.-L. Han, Network-based $\mathcal{H}_\infty$ filtering using a logic jumping-like trigger, Automatica 49 (5) (2013) 1428–1435, http://dx.doi.org/10.1016/j.automatica.2013.01.060.
[26] B.-L. Zhang, Q.-L. Han, X.-M. Zhang, Event-triggered $\mathcal{H}_\infty$ reliable control for offshore structures in network environments, J. Sound. Vib. 368 (2016) 1–21, http://dx.doi.org/10.1016/j.jsv.2016.01.008.
[27] H. Du, N. Zhang, Control for buildings with time delay in control via linear matrix inequalities and genetic algorithms, Eng. Struct. 30 (1) (2008) 81–92, http://dx.doi.org/10.1016/j.engstruct.2007.03.005.
[28] Y. Chen, W. Zhang, H. Gao, Finite frequency $\mathcal{H}_\infty$ control for building under earthquake excitation, Mechatronics 20 (1) (2010) 128–142, http://dx.doi.org/10.1016/j.mechatronics.2009.11.001.
[29] B. Zhu, W. Lin, Q. Zhan, W. Sun, T. Hayat, F. Alsaadi, Active fault tolerant control of buildings for seismic loads in finite frequency domain, J. Frankl. Inst. 352 (10) (2015) 4247–4262, http://dx.doi.org/10.1016/j.jfranklin.2015.06.013.
[30] K. Miyamoto, J. She, J. Imani, X. Xin, D. Sato, Equivalent-input-disturbance approach to active structural control for seismically excited buildings, Eng. Struct. 125 (2016) 392–399, http://dx.doi.org/10.1016/j.engstruct.2016.07.028.
[31] W. Zhang, Y. Chen, H. Gao, Energy-to-peak control for seismic-excited buildings with actuator faults and parameter uncertainties, J. Sound. Vib. 330 (4) (2011) 581–602, http://dx.doi.org/10.1016/j.jsv.2010.09.001.
[32] E. Fridman, A. Seuret, J.-P. Richard, Robust sampled-data stabilisation of linear systems: an input delay approach, Automatica 40 (8) (2004) 1441–1446, http://dx.doi.org/10.1016/j.automatica.2004.03.003.
[33] R. Sakthivel, S. Santra, K. Mathiyalagan, S. Anthoni, Robust reliable sampled-data control for offshore steel jacket platforms with nonlinear perturbations, Nonlinear Dyn. 78 (2) (2014) 1109–1123, http://dx.doi.org/10.1007/s11071-014-1500-4.
[34] R. Sakthivel, P. Selvaraj, K. Mathiyalagan, J. Park, Robust fault-tolerant $\mathcal{H}_\infty$ control for offshore steel jacket platforms via sampled-data approach, J. Frankl. Inst. 352 (6) (2015) 2259–2279, http://dx.doi.org/10.1016/j.jfranklin.2015.03.016.
[35] X.-M. Zhang, Q.-L. Han, X. Yu, Survey on recent advances in networked control systems, IEEE Trans. Ind. Inf. 12 (5) (2016) 1740–1752, http://dx.doi.org/10.1109/TII.2015.2506545.
[36] L. Hetel, C. Fiter, H. Omran, A. Seuret, E. Fridman, J.-P. Richard, S.I. Niculescu, Recent developments on the stability of systems with aperiodic sampling: an overview, Automatica 76 (2017) 309–335, http://dx.doi.org/10.1016/j.automatica.2016.10.023.
[37] X.-M. Zhang, Q.-L. Han, D. Han, Effects of small time-delays on dynamic output feedback control of offshore steel jacket structures, J. Sound. Vib. 330 (16) (2011) 3883–3900, http://dx.doi.org/10.1016/j.jsv.2011.03.023.
[38] S. Boyd, L. El Ghaoui, E. Feron, V. Balakrishnan, Linear Matrix Inequalities in System and Control Theory, SIAM, 1994. https://books.google.com/books?isbn=0898714850.
[39] X.-M. Zhang, Q.-L. Han, Event-triggered H∞ control for a class of nonlinear networked control systems using novel integral inequalities, Int. J. Robust Nonlin. Control 27 (4) (2017)679–700, http://dx.doi.org/10.1002/rnc.3598.
[40] X.-M. Zhang, Q.-L. Han, A decentralized event-triggered dissipative control scheme for systems with multiple sensors to sample the system outputs, IEEE Trans. Cybern. 46 (12) (2016) 2745–2757, http://dx.doi.org/10.1109/TCYB.2015.2487420.
[41] B.-L. Zhang, M. Meng, Q.-L. Han, X.-M. Zhang, Robust non-fragile sampled-data control for offshore steel jacket platforms, Nonlinear Dyn. 83 (4) (2016) 1939–1954, http://dx.doi.org/10.1007/s11071-015-2457-7.